Increasing the sensitivity of controlled source electromagnetics by using synthetic aperture

Y. Fan[1], R. Snieder[1], E. Slob[1,2], J. Hunziker[2], J. Singer[3], J. Sheiman[3] & M. Rosenquist[3]

[1] *Center for Wave Phenomena, Colorado School of Mines, Golden, USA*
[2] *Section of Applied Geophysics and Petrophysics, Department of Geotechnology, Delft University of Technology, Delft, The Netherlands*
[3] *Shell International Exploration & Production, Houston, USA*

ABSTRACT

Controlled-source electromagnetics (CSEM) has been used as a de-risking tool in the hydrocarbon exploration industry. Although there have been successful applications of CSEM, this technique is still not widely used in the industry because the limited types of hydrocarbon reservoirs CSEM can detect. In this paper, we apply the concept of synthetic aperture to CSEM data. Synthetic aperture allows us to design sources with specific radiation patterns for different purposes. The ability to detect reservoirs is dramatically increased after forming an appropriate synthetic aperture antenna. Consequently, the types of hydrocarbon reservoirs that CSEM can detect are significantly extended. In this paper, we mainly show one type of synthetic aperture antenna whose field can be steered into a designed angle. Consequently, the field concentrates on the target reservoir and the airwave is reduced. We show a synthetic example and a data example to illustrate the increased sensitivity obtained by applying synthetic aperture CSEM source. Because synthetic apertures are constructed as a data processing step, there is no additional cost for the CSEM acquisition. Aside from the applications to marine CSEM, synthetic aperture can be widely applied to other electromagnetic methods such as on land electromagnetics and bore hole electromagnetics.

Introduction

After the development in academia starting in the late 1970s (Spiess et al. 1980; Cox 1981; Young and Cox 1981) and the early industry experiments (Srnka 1986; Constable et al. 1986; Chave et al. 1991; Hoversten and Unsworth 1994), CSEM was introduced to the industry at the beginning of this century as a method to explore hydrocarbons. Since then the research and commercial surveys on CSEM have boomed (Constable and Srnka 2007; Chopra et al. 2007).

The fundamental concept and the assumption of using CSEM as a detector of hydrocarbons is that porous rocks are resistive when they are saturated with gas or oil (Edwards 2005; Constable and Srnka 2007). In a standard CSEM survey, a horizontal current dipole is used as the source to generate an electromagnetic field and is towed close to the sea floor to avoid energy loss in the conductive sea water. The receivers are located on the sea floor. A resistive hydrocarbon reservoir in the subsurface (a target with a resistivity of approximate 50 to 100 Ωm) embedded in the conductive background (about 1 Ωm), acts as a secondary source that refracts the electromagnetic field back to the receivers. In this way, one can infer the presence of a resistive body in the subsurface from the measured electromagnetic field.

The main challenge of CSEM is the diffusive nature of electromagnetic field in the conductive subsurface. Thus the secondary field that refracts from the target is significantly small at most of the offsets than the field which does not carry any information of the subsurface, such as the direct arrival and the air wave, (Edwards 2005; Constable and Srnka 2007). So it is not surprise that most of the successful CSEM applications are in the deep water environment (deeper than 1km) with the shallow target (less than 3km).

We introduce the concept of synthetic aperture to CSEM data. Synthetic aperture allows us to design

sources with specific radiation patterns for different purposes. Here we construct a synthetic aperture antenna to steer the electromagnetic field into a designed direction (Note that the use of synthetic aperture is not limited to field steering). By doing this, one can concentrate the energy into a direction where the target is located. At the same time, the air wave can be significantly reduced by increasing the propagation path in the sea water. Consequently, the ability to detect the reservoirs is dramatically increased after applying appropriate synthetic apertures without any cost increase. Aside from the applications to CSEM, synthetic aperture can be widely applied to other electromagnetic methods such as CSEM on land and bore hole electromagnetics.

1 SYNTHETIC APERTURE METHOD

Although synthetic aperture is a widely used concept for waves such as radar and sonar (Barber 1985; Ralston et al. 2007; Zhou et al. 2009; Cutrona 1975; Riyait et al. 1995; Bellettini and Pinto 2002), to the best of the authors' knowledge, this is the first time that synthetic aperture is introduced to a diffusive field like CSEM.

A general formula for constructing a synthetic aperture S_A is

$$S_A(x,\omega) = \sum_{n=1}^{N} a_n e^{i\phi_n} s(x, x_n, \omega). \quad (1)$$

At a single angular frequency ω, a synthetic aperture at location x is a superposition of the sequentially distributed sources that are located from x_1 to x_N with an amplitude weighting a_n and a phase shift ϕ_n. The source function for the individual source is represented by $s(x, x_n, \omega)$. For example, a horizontal 100 m dipole source centered at x_n with a current of 100 A and a frequency of 1 Hz can be represented by

$$s(x, x_n, \omega) = \begin{cases} 100\ A & (x_n - 50 < x < x_n + 50), \\ 0 & (otherwise). \end{cases} \quad (2)$$

Using the combination of amplitude weighting and a phase shift for sequential sources, enables us to propagate the field with a specific radiation pattern. For example, with a linear phase shift, the field can be steered into a certain direction as illustrated in figure 1. The larger semicircle represents the field whose source starts earlier (smaller value of ϕ_n in frequency domain); while the smaller one is from the source that starts later (larger value of ϕ_n in frequency domain). In this particular example, the total field is steered from the vertical direction to the right by applying a linear phase shift to individual sources.

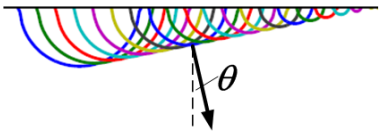

Figure 1. Field steering by applying a linear phase shift

2 SYNTHETIC AND FIELD DATA EXAMPLE

2.1 Synthetic data example

In the numerical model shown we use a hydrocarbon reservoir (5km in the x and y directions with a thickness of 100 m) located 1 km below the sea floor. The sea water is 1km deep with a resistivity of 0.3 Ωm. The subsurface background is a half space with a resistivity of 1 Ωm. The resistivity of the reservoir is set to be 100 Ωm. The receivers are located at the sea floor and a 100 m dipole source with a current of 100 A is continuously towed 100 m above the receivers. Although only the inline electrical field E_x is discussed in this paper, the synthetic aperture principle holds for the other components of the electrical and magnetic fields as well.

In this example, we focus on the construction of a synthetic aperture with the field steered toward the target direction. Figure 2(a) shows the inline electrical fields with the reservoir (dashed line) and without the reservoir (solid line) from a single 100 m dipole whose center is located at x =-6.5 km. There is a slight increase in the field around the position x=0 km when the reservoir is present. This 20% difference is shown by the ratio of the field with the reservoir to the field without the reservoir (black solid curve in figure 2(e)).

Simply superposing the 50 (N=50 in equation 1) employed sequential sources, is equivalent to setting the weighting function a_n=1 and ϕ_n=0 in equation 1. This superposition gives a 5 km long dipole source with a current of 100 A. The total E_x field is given by figure 2(b). The ratio of the fields with and without the reservoir is shown by the red dashed curve in panel (e). Although the overall signal strength increases compared to the single 100 m source (panel (a)), the difference between the models with and without the reservoir does not significantly increase by simply using a longer dipole.

Instead of using a zero phase shift in equation 1, we next apply a linear phase shift to the sequential sources using $\phi_n = c_1 k_r n \Delta s$, where Δs is the distance between the centers of two neighboring sources, k_r is the real part of the complex wave number and c_1 is a coefficient to control how much the field is steered. The steering angle θ (as defined in figure 1) is related to this coefficient by $c_1 = sin\theta$. As shown in figure 1, this phase shift effectively deploys the sources on the left at an earlier time than those on the right. Consequently, the total field propagates toward the right. Figure 2(c) shows the Ex field excited by this new synthetic aperture source.

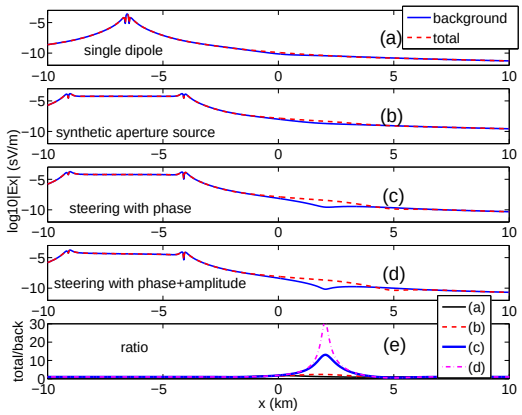

Figure 2. Panels (a) to (d) show the inline electrical fields with the reservoir (dashed lines) and without the reservoir (solid) for four different sources; a 100 m dipole source (panel (a)); a 5 km dipole source (panel (b)); a 5 km synthetic source obtained from field steering toward the target by the phase shift (panel (c)); A 5 km synthetic source obtained from field steering toward the target by the phase shift and the amplitude compensation (panel (d)). Panel (e) shows the ratio between the fields with and without the reservoir. The four curves in panel (e) represent the ratios from each of the panels above.

The ratio of the steered fields is illustrated by the blue solid curve in the bottom panel. This example shows that the detectability significantly increases by steering the field toward the target.

There are two reasons for the improved detectability. First, the total electrical field as well as the z component of the E field increases at the target location when the field propagation is steered from the vertical direction to a tilted angle. The z component of the E field diagnoses changes in the conductivity in the vertical direction (Edwards 2005). The second reason is the reduction of the background field. We will investigate the mechanism of the background field reduction in the future.

Although we already see the improvement of field steering with linear phase shift. The high decay factor makes the steering of the diffusive field not accurate by only using phase shift. The attenuation of a diffusive field, causes the sources on the left side to give a smaller contribution to the synthetic aperture construction because they propagates longer. These sources are indicated by the bigger semicircles in figure 1. In order to have a more effective steered field, we use an energy compensation term $a_n = e^{-c_2 k_i n \Delta s}$, where c_2 is a constant that controls the amplitude weighting. In this particular example, c_2 is chosen to be 0.1 m^{-1} as an empirical value that gives a maximum response.After we include this energy compensation, the difference between the models with and without the target further increases, as shown in figure 2(d). This difference is quantified by the ratio of the fields with and without the target and is illustrated by the magenta dashed line in panel (e).

The examples show that the synthetic aperture technique dramatically increases the difference in electrical field response between the models with and without the reservoir by a factor of 30. Note that this is achieved without altering the data acquisition. If noise is added in the above example, the main observation still holds. But we can not steer the field as effective as the noise free data and therefore the anomaly ratio is not as big as the factor of 30. We also see the effect of noise in the real data example below.

2.2 Real data example

Next, we apply this steering concept to the real data. In the real data, the field 'without' the target is defined as the measured field at a reference site under which there is no reservoir. For a standard single dipole measurement, the inline electrical fields with and without the reservoir are shown by the pink and black solid curves, respectively, in the upper panel of figure 3. The corresponding ratio of the two fields is shown by the solid curve in the lower panel of figure 3. The reservoir is known to be located between x=3 km and x=6 km. A slight difference in the electrical field can be observed between the offset of 6 km and 10 km due to the presence of the reservoir. Beyond the offset of 10 km, the ratio oscillates because the field reaches the noise level. This oscillation makes it difficult to interpret the data.

Next, we construct a 4 km synthetic aperture source with no field steering (zero phase shift). The fields with and without the reservoir are shown by the pink and black dashed curves in the upper panel of figure 3, respectively, and the corresponding ratio is the dashed curve in the lower panel. Because the longer dipole source has a better signal to noise ratio (the signal is stronger), both the Ex field (upper panel) and the ratio (lower panel) are smoother than the field generated by an individual source . The overall difference between the models, however, does not change too much.

As we did in the synthetic example, next we construct a 4km synthetic aperture source with field steering toward the reservoir using a phase shift ($c_1 = 0.8$) and amplitude weighting ($c_2 = 0.7\ \mathrm{m}^{-1}$). Figure 4 shows that the difference between the models has significantly increased after we apply the field steering. One can be more confident to infer the presence of the reservoir from figure 4 than from figure 3. Note that the negative offset does not show any difference in the field both before and after the field steering as we expect. This is because there is no reservoir on the negative offset side. At the same time, the consistency on the negative offset

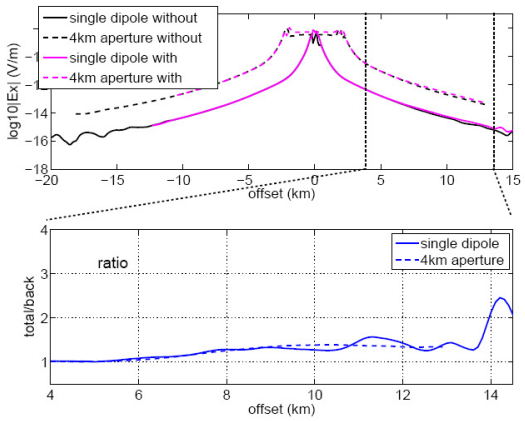

Figure 3. Upper panel: inline electrical field with the reservoir (pink lines) and without the reservoir (black lines) from a single dipole (solid lines) and 4 km synthetic aperture (dashed lines) without the field steering. Lower panel: ratio of the field with the reservoir to the field without the reservoir from the single dipole (solid lines) and the synthetic aperture (dashed lines).

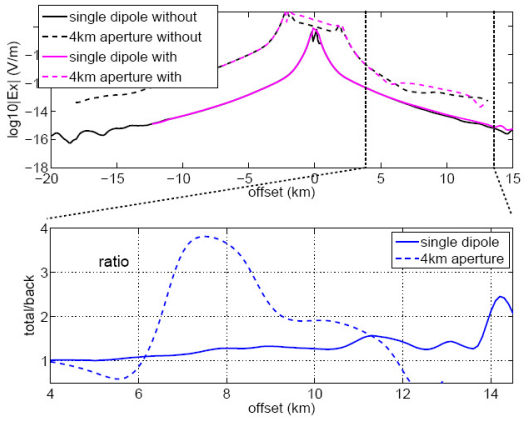

Figure 4. Upper panel: inline electrical field with the reservoir (pink lines) and without the reservoir (black lines) from a single dipole (solid lines) and 4 km synthetic aperture (dashed lines) with the field steering toward the reservoir. Lower panel: ratio of the field with the reservoir to the field without the reservoir from the single dipole (solid lines) and the synthetic aperture (dashed lines).

side, where there is no reservoir, confirms that our field steering is only sensitive to the presence of the reservoir.

3 DISCUSSION AND CONCLUSION

The synthetic aperture technique opens a new line of research in CSEM data processing. Hidden information in CSEM data can be retrieved by using the synthetic aperture technique with little extra cost because there is no need to change the acquisition. The ability to detect the reservoirs is dramatically increased after applying appropriate synthetic apertures. The depth of the reservoir that CSEM detects can also increase with the use of synthetic aperture methods. Consequently, the types of hydrocarbon reservoirs that CSEM can detect are extended. Other types of synthetic aperture, aside field steering, can be designed, e.g. field focusing and the synthetic vertical source. In this paper, we only show examples of constructing synthetic aperture source in a line (2D synthetic aperture). In principle, one can construct 3D synthetic aperture to better detect the 3D structure of the subsurface. For example, when data are collected with antennas along parallel lines, one not only can steer the field in the inline direction, but also in the crossline direction. The synthetic aperture technique is not limited to the source side. It can also be applied to the receiver side by the same principle. Besides the application to the current marine CSEM system, synthetic aperture can also be used in land surveys and bore hole applications.

4 ACKNOWLEDGMENTS

The authors are grateful for the financial support through a Shell Gamechanger Project. The electromagnetic research team in Shell provided technical support in the research and we thank them for the permission for using the real data.

REFERENCES

Barber, B. C., 1985, Theory of digital imaging from orbital synthetic-aperture radar: Int. J. Remote Sens., **6**, 1009–1057.

Bellettini, A. and M. Pinto, 2002, Theretical accuracy of synthetic aperture sonar micronavigation using a displaced phase-center antenna: IEEE J. Oceanic Eng., **27**.

Chave, A. D., S. C. Constable, and R. N. Edwards, 1991, Electrical exploration methods for the seafloor, *in* M. Nabighian ed., Electromagnetic methods in applied geophysics, volume **2**, 931–966, SEG.

Chopra, S., K. Strack, C. Esmersoy, and N. Allegar, 2007, Introduction to this special section: CSEM: The Leading Edge, **26**, 323–325.

Constable, S. and L. J. Srnka, 2007, An introduction to marine controlled-source electromagnetic methods for hydrocarbon exploration: Geophysics, **72**, WA3–WA12.

Constable, S. C., C. S. Cox, and A. D. Chave, 1986, Offshore electromagnetic surveying techniques: SEG Expanded Abstracts, **5**, 81–82.

Cox, C. S., 1981, On the electrical conductivity of the oceanic lithosphere: Physics of The Earth and Planetary Interiors, **25**, 196–201.

Cutrona, L., 1975, Comparison of sonar system performance achievable using synthetic-aperture techniques with the performance achievable by more conventional means: J. Acoust. Soc. Am., **58**, 336–348.

Edwards, N., 2005, Marine controlled source electromagnetics: Principles, methodologies, future commercial applications: Surveys in Geophysics, **26**, 675–700.

Hoversten, G. M. and M. Unsworth, 1994, Subsalt imaging via seaborne electromagnetics: Offshore Technology Conference, **26**, 231–240.

Ralston, T. S., D. L. Marks, C. P. Scott, and S. A. Boppart, 2007, Interferometric synthetic aperture microscopy: Nature Physics, **3**, 129–134.

Riyait, V., M. Lawlor, A. Adams, O. Hinton, and B. Sharif, 1995, Real-time synthetic aperture sonar imaging using a parallel architecture: Image Processing, IEEE Transactions on, **4**, 1010–1019.

Spiess, F. N., K. C. Macdonald, T. Atwater, R. Ballard, A. Carranza, D. Cordoba, C. Cox, V. M. D. Garcia, J. Francheteau, J. Guerrero, J. Hawkins, R. Haymon, R. Hessler, T. Juteau, M. Kastner, R. Larson, B. Luyendyk, J. D. Macdougall, S. Miller, W. Normark, J. Orcutt, and C. Rangin, 1980, East Pacific Rise: Hot springs and geophysical experiments: Science, **207**, 1421–1433.

Srnka, L. J., 1986, Method and apparatus for offshore electromagnetic sounding utilizing wavelength effects to determine optimum source and detector positions: U.S. Patent 4,617,518.

Young, P. D. and C. S. Cox, 1981, Electromagnetic active source sounding near the east pacific rise: Geophys. Res. Lett., **8**, 1043–1046.

Zhou, X., N. Chang, and S. Li, 2009, Applications of SAR interferometry in earth and environmental science research: Sensors, **9**, 1876–1912.